Structure and shape of nematic liquid crystal microdroplets
by Wei Huang

A thesis submitted in partial fulfillment of the requirements for the degree of Master of Science in Physics
Montana State University

Abstract:
With a numerical relaxation method and Landau-de Gennes theory, we have calculated the continuous dependence of structure and shape of tangentially anchored liquid crystal microdroplets on the parameters of anchoring strength W0 and radius r, at. fixed temperature. The structure is characterized by order parameter field S and director field n and the shape is described by a prolateness parameter x. For structure, we find that there exists an order/disorder first-order transition induced by r, a distortion/uniform first-order transition of S induced by w0, and a distortion/uniform continuous transition of n induced by both W0 and r. For shape, we find that the change of bulk free energy due to deviations from spherical shape can never compete with that of the surface energy. The surface interaction itself can induce prolateness, which becomes greater and approaches to a limiting value as the size gets smaller, and which is almost proportional to W0/ς None of the above predictions have been reported before. Our physical explanations show they are reasonable and not the outcomes of approximations made in the work.

STRUCTURE AND SHAPE OF NEMATIC LIQUID CRYSTAL MICRODROPLETS

by

Wei Huang

A thesis submitted in partial fulfillment
of the requirements for the degree

of

Master of Science

in

Physics

MONTANA STATE UNIVERSITY
Bozeman, Montana

April 1993

APPROVAL

of a thesis submitted by

Wei Huang

This thesis has been read by each member of the thesis committee and has been found to be satisfactory regarding content, English usage, format, citations, bibliographic style, and consistency and is ready for submission to the College of Graduate Studies.

4-23-93
Date

George Twitchell
Chairman, Graduate Committee

Approved for the Major Department

4-27-93
Date

Head, Major Department

Approved for the College of Graduate Studies

5/17/93
Date

Graduate Dean

STATEMENT OF PERMISSION TO USE

In presenting this thesis in partial fulfillment of the requirements for a master's degree at Montana State University, I agree that the Library shall make it available to borrowers under rules of the Library.

If I have indicated my intention to copyright this thesis by including a copyright notice page, copying is allowable only for scholarly purposes, consistent with "fair use" as prescribed in the U.S. Copyright Law. Requests for permission for extended quotation from or reproduction of this thesis in whole or in parts may be granted only by the copyright holder.

Signature 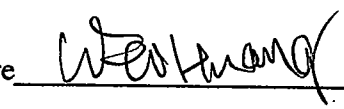

Date 4/20/93

TABLE OF CONTENTS

LIST OF TABLES

LIST OF FIGURES

ABSTRACT

With a numerical relaxation method and Landau-de Gennes theory, we have calculated the continuous dependence of structure and shape of tangentially anchored liquid crystal microdroplets on the parameters of anchoring strength w_0 and radius r, at fixed temperature. The structure is characterized by order parameter field S and director field **n** and the shape is described by a prolateness parameter x. For structure, we find that there exists an order/disorder first-order transition induced by r, a distortion/uniform first-order transition of S induced by w_0, and a distortion/uniform continuous transition of **n** induced by both w_0 and r. For shape, we find that the change of bulk free energy due to deviations from spherical shape can never compete with that of the surface energy. The surface interaction itself can induce prolateness, which becomes greater and approaches to a limiting value as the size gets smaller, and which is almost proportional to w_0/σ. None of the above predictions have been reported before. Our physical explanations show they are reasonable and not the outcomes of approximations made in the work.

CHAPTER 1

INTRODUCTION

There has been continuous interest in liquid crystals (LC) over the past several decades due to their importance in the electro-optic industry. Studies of a LC microdroplet have been stimulated recently by the appearance of a new generation of LC shutters and displays based on the use of polymer-dispersed liquid crystals (PDLC) [1]. A PDLC is a solid polymer in which a large number of LC droplets, whose radii vary from the submicrometer region up to 100 μm, are embedded.

Basic Knowledge about LCs

A liquid crystal is one of the intermediate phases between phases of crystalline solid and isotropic liquid. These intermediate phases are called mesophases. We can briefly say that LCs are ordered fluid mesophases, compared to plastic crystals which are disordered solid mesophases. A liquid crystal can flow like an ordinary liquid, while other properties, for example the birefringence, are reminiscent of those of a crystalline phase. Liquid crystals are characterized by the fact that the molecular translational order has disappeared, while some degree of orientational order is still present. (By contrast, plastic

crystals have translational order but not orientational order.) Usually the molecules of LC are greatly elongated ones, and their long axes, except for the influence of thermal fluctuations, are parallel to each other.

There are two types of LC, thermotropic and lyotropic. The term "thermotropic" arises because transitions involving these mesophases are most naturally effected by changing temperature. This type is of interest both from the standpoint of basic research and for applications in electro-optic displays, etc. We deal with this type in our work. Solutions of rod-like entities in a normally isotropic solvent often form LC phases for sufficiently high solute concentration. These anisotropic solution mesophases are called "lyotropic" LC. The natural parameter inducing phase transitions of this type is the solute concentration. Lyotropic LCs are of interest in polymer and biological studies.

Liquid crystals can be classified as nematic and smectic according to molecular order, as Fig.1 shows. Under each type there are several subtypes, e.g., cholesteric nematic, smectic A, smectic B, etc. The essential difference between a nematic LC and a smectic LC is that the smectic phase has some degree of positional order, i.e., layering.

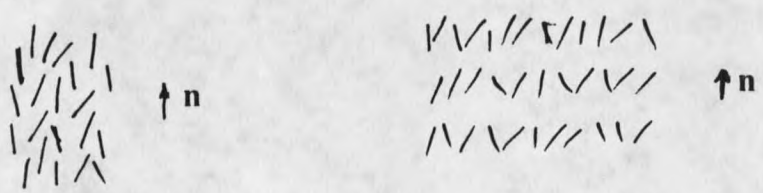

Figure 1. Schematic picture of the nematic (a) and smectic A (b) phase.

Molecular statistical theory and macroscopic continuum theory are used to describe the structures and properties of LC. Macroscopically in most cases we use two structural quantities, a unit vector **n** (the director) and a scalar S (the order parameter). **n** is the local average direction of molecular axes. S measures the local average deviation of directions of molecular axes from **n**. More general quantities will be described in Chapter 2.

In the commonly used macroscopic elastic continuum theory which embeds the order parameter into temperature dependent elastic constants, there are three independent distortion modes of director field (Fig. 2), and the free energy density is

$$f = \frac{1}{2}\left[K_{11}(\nabla\cdot\boldsymbol{n})^2 + K_{22}(\boldsymbol{n}\cdot\nabla\times\boldsymbol{n})^2 + K_{33}(\boldsymbol{n}\times\nabla\times\boldsymbol{n})^2\right] \qquad (1)$$

where the so-called Frank elastic constants K_{11}, K_{22}, and K_{33} are, respectively, the splay, twist, and bend elastic constants.

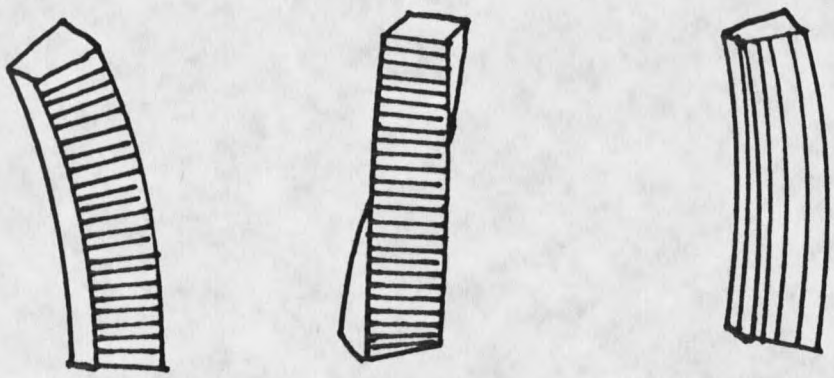

(a) (b) (c)

Figure 2. The three basic deformations of a uniaxial nematic: (a) splay, (b) twist, (c) bend.

At the interface between a LC and other phase, anchoring always occurs, even if the other phase is vacuum. Anchoring means there is a preferable direction for the director **n** at the interface. The simplest way to describe anchoring is shown by equation (2) for the surface energy density:

$$f_s = \sigma - \frac{1}{2} w_0 \cos^2(\alpha \cdot \beta) \qquad (2)$$

α and β are respectively, the favorable direction unit vector and the actual surface director. Depending on the materials, α can vary from tangential to the surface to normal to the surface. σ and w_0 are the surface tension constant and the anchoring strength parameter, respectively.

There are several types of structures for nematic LC droplets which reflect two typical boundary anchoring condition: tangential and normal (Fig.3). The characterization of these types is by the different distortion patterns of director **n** field.

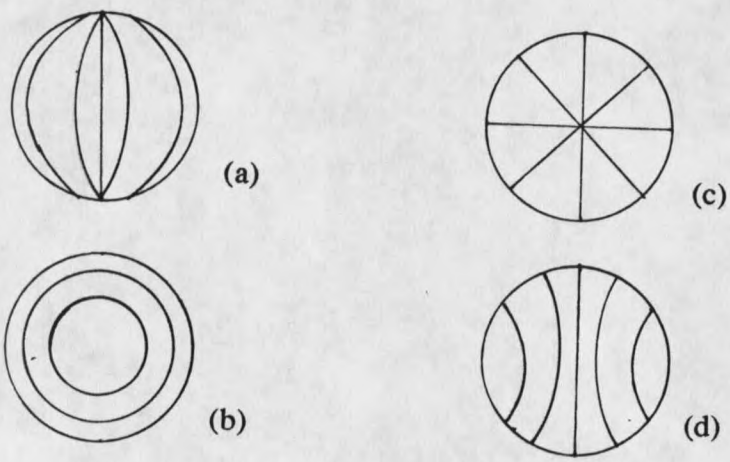

Figure 3. Director configurations in nematic microdroplets:

(a) bipolar, (b) toroidal, (c) radial, and (d) axial structures.

Review of Other Work

The previous theoretical work on the subject can be divided into following categories.

(1) Obtaining one of the above structures [2][3].

(2) Studying the nematic/isotropic transition of certain structures for the LC droplets as the temperature varies [4][5]. For example, in [5] Zumer et al. showed the director and order parameter configuration for a bipolar droplet near the nematic/isotropic phase transition, with a strong anchoring condition.

(3) Studying the transition between two of these structures, as external field or ratio of elastic constants varies [6][7]. For example, in [7] R.D.Williams calculated the transition of the bipolar/twist-bipolar configuration, occurring when $K_{11} > K_{22}+0.431K_{33}$.

Computational relaxation methods and Landau-de Gennes theory are the common tools of these works. The agreement between experiment and theoretical calculation [9][10] stand as the support for the appropriateness of the theory.

However, a clear and integral picture of LC droplet structure's continuous dependence

on various parameters is still missing, especially for submicrometer droplets and for droplets with three different elastic constants. Furthermore until this thesis no work on the shape of LC microdroplets has been carried out.

Introduction of this Work

In this thesis, we study with a numerical relaxation method, the structure and shape of tangentially anchored droplets with one-elastic-constant and no-twist approximations, probing their continuous dependencies on radius, anchoring strength, etc., followed by physical explanations.

CHAPTER 2

LANDAU-DE GENNES THEORY AND THE PROBLEM OF THIS STUDY

Tensor Order Parameter

A nematic LC state is characterized by an macroscopic second rank tensor order parameter **Q**. A macroscopic approach can be used in constructing **Q**, i.e., the construction is independent of any assumption regarding the molecules. Consider the application of some field **X** on the system with a response **Y** given by:

$$Y_\alpha = T_{\alpha\beta} X_\beta \qquad (3)$$

where $T_{\alpha\beta}$ is a symmetric tensor. As an example **X** and **T** may represent respectively the external magnetic field **B** and the susceptibility tensor χ, and $\mu_0^{-1}\mathbf{Y}$ is the magnetization **M**.

In a properly chosen coordinate system, **T** is diagonal:

$$\mathbf{T}=\begin{bmatrix} T_1 & 0 & 0 \\ 0 & T_2 & 0 \\ 0 & 0 & T_3 \end{bmatrix} \qquad (4)$$

A tensor order parameter is obtained by extracting the anisotropic part of **T**. This can be accomplished by putting $\Sigma T_i = T$, then letting the diagonalized order parameter tensor **Q**

be:

$$\mathbf{Q}=\begin{bmatrix} -1/3(Q_1-Q_2) & 0 & 0 \\ 0 & -1/3(Q_1+Q_2) & 0 \\ 0 & 0 & 2/3Q_1 \end{bmatrix} \tag{5}$$

where Q_1 and Q_2 are determined by:

$$T_1=1/3T\ (1-Q_1+Q_2) \tag{6}$$

$$T_2=1/3T\ (1-Q_1-Q_2) \tag{7}$$

$$T_3=1/3T\ (1+2Q_1) \tag{8}$$

Q_1 and Q_2 have values between 0 and 1. The isotropic liquid is described by $Q_1=Q_2=0$. The anisotropic liquid with uniaxial symmetry is described by only one order parameter. In this case the unique axis is conventionally chosen along the basis vector e_3 and the medium is described by $Q_1\neq0$ and $Q_2=0$. (A perfectly aligned medium has $Q_1=1$.) Changing the uniaxial symmetry into a biaxial one requires the introduction of the second independent order parameter Q_2. Clearly the order parameter **Q** depends on the temperature.

The general expression for the tensor order parameter is obtained by an arbitrary rotation of the coordinate system.

$$Q_{\alpha\beta} = -\frac{1}{3}(Q_1 - Q_2)(e_\alpha \cdot e_1')(e_\beta \cdot e_1') - \frac{1}{3}(Q_1 + Q_2)(e_\alpha \cdot e_2')(e_\beta \cdot e_2') + \frac{2}{3}Q_1(e_\alpha \cdot e_3')(e_\beta \cdot e_3') \quad (9)$$

where e_α' is the cartesian coordinate system giving rise to a diagonal representation of Q, and e_α is the new coordinate system.

Induction of S and n from Q

For nematics with uniaxial symmetry, the direction of the unique axis, which is given by the director n, coincides with one of the basis vectors belonging to the cartesian coordinate system in which Q is diagonal. And diagonized Q is written as

$$Q = S \begin{pmatrix} -1/3 & 0 & 0 \\ 0 & -1/3 & 0 \\ 0 & 0 & 2/3 \end{pmatrix} \quad (10)$$

where S is the scalar order parameter and is equal to Q_1 of equation (5). In an arbitrary external coordinate system,

$$Q_{ij} = \frac{1}{3}S(3n_i n_j - \delta_{ij}) \quad (11)$$

Relationship Between Macroscopic Order Parameter and Microscopic Orientational Order of Molecules

It can be shown for a nematic LC composed of rod-like molecules [11],

$$\boldsymbol{n}(r) = \langle \boldsymbol{a}(r) \rangle \tag{12}$$

$$S(r) = \frac{1}{2}\langle 3\cos^2\theta - 1 \rangle \tag{13}$$

where **a** is direction of an individual molecule, θ is the angle between **a** and **n**, and <...> represents a local thermal average.

If the distribution of the long molecular axes is random, as in the isotropic phase, we have $\langle \cos^2\theta \rangle = 1/3$, and S=0. The value S=1 corresponds to the case of perfectly aligned molecules.

Landau-de Gennes Theory of Free Energy and Phase Transition

In 1937 Landau speculated that near a first or second-order phase transition point the free energy density function can be expanded as a power series in the order parameter and its spatial derivatives, with temperature-dependent coefficients. He further argued that only the leading terms of the series are important, so that the expansion of the free energy density function becomes a simple low order polynomial in the order parameters. Landau's theory of phase transitions has proven to be as good as mean field theory in

providing a semi-quantitative description of the specific heat, the order parameter, and the entropy in the vicinity of phase transition. De Gennes was the first to successfully apply Landau's theory to first-order LC phase transitions.

The Landau free energy density expression for a nematic LC, constructed with order parameter tensor Q is:

$$f=f_0+\frac{1}{2}a(T-T_c^*)Q_{ij}Q_{ji}+\frac{1}{3}BQ_{ij}Q_{ki}+\frac{1}{4}C_1(Q_{ij}Q_{ji})^2$$

$$+\frac{1}{4}C_2Q_{ij}Q_{jk}Q_{kl}Q_{li}+\frac{1}{2}L_1\partial_i Q_{jk}\partial_i Q_{jk}+\frac{1}{2}L_2\partial_i Q_{ij}\partial_k Q_{kj} \qquad (14)$$

where f_0(T) is the free energy density of the isotropic phase; T_c^* is a temperature slightly below the bulk sample transition temperature T_c. (T_c^* can be interpreted physically as that temperature below which supercooling becomes impossible.) The parameters a,B,C_1,C_2,L_1,L_2 are temperature-independent bulk material constants. With substitution of equation (10), constants C_1 and C_2 can be combined to $C=C_1+C_2/2$. L_1 and L_2 are two independent elastic constants. It should be noted that in the nematic phase there are known to be three independent elastic constants, and the Landau expansion to the second order gives rise to two of them.

Our Problem

In our work we use equal-elastic constant approximation, and f becomes:

$$f_b(r,T) = f_0 + \frac{1}{2}a(T-T^*)S^2 - \frac{1}{3}BS^3 + \frac{1}{4}CS^4 + \frac{3}{4}L_1(\nabla S)^2$$

$$+\frac{9}{4}S^2L_1[(\nabla\cdot\boldsymbol{n})^2 + (\nabla\times\boldsymbol{n})^2] \qquad (15)$$

The relationship between L_1 and the Franck elastic constant K is $L_1 = 2K/(9S^2)$.

The droplet we are studying has cylindrical symmetry, so, assuming no twist, **n** can be expressed by the scalar angle θ (Fig.4), and f becomes,

$$f(\rho,z,T) = f_0 + \frac{1}{2}a(T-T^*)S^2 - \frac{1}{3}BS^3 + \frac{1}{4}CS^4 + \frac{3}{4}L_1[(\partial S/\partial\rho)^2 + (\partial S/\partial z)^2]$$

$$+\frac{9}{4}S^2L_1[\frac{1}{\rho^2}\sin^2\theta + (\partial\theta/\partial\rho)^2 + (\partial\theta/\partial z)^2 + \frac{2}{\rho}\sin\theta\cos\theta(\partial\theta/\partial\rho) + \frac{2}{\rho}\sin^2\theta(\partial\theta/\partial z)] \qquad (16)$$

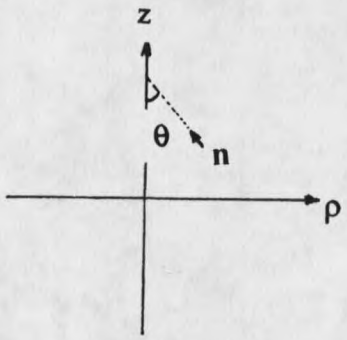

Figure 4. Description of the local director **n** in the droplet.

z is the axis of cylindrical symmetry of the droplet.

The problem is that of the minimization of the total free energy, which is the sum of the integrals of the above bulk term, and the surface term of equation (2).

An open question is the shape of a freely suspended LC droplet. Here "free" means the environment is an isotropic fluid. We can approach the problem qualitatively in the following way. The first consideration is dimensional analysis. Since the bulk elastic energy density is associated with the squares of gradients of **n**, the elastic energy of a volume of nematic is proportional to the linear dimension L of the droplet. On the other hand, the surface energy is proportional to L^2. Thus the internal energy of a large drop is dominated by the surface energy, and the drop is spherical. For small drops, the bulk energy can dominate, and due to preference of an elongated shape of the bulk, the shape may be nonspherical. The other consideration is that, for weak surface anchoring, the surface energy itself may tend to be smaller for an elongated shape.

There are experimental optical photographs of free LC droplets bigger than 1 μm, which are spherical, but no experiment or theory on the shapes for smaller droplets exists in the literature, to our knowledge. Since computational results show that the effect of deviation from sphere is small, through our work we can simply study prolate shapes, of course including the sphere.

CHAPTER 3

NUMERICAL METHOD

Usual Method

Usually when one solves a minimization problem, one uses a variational method to get a set of Euler-Lagrange partial differential equations. In this problem, for a fixed shape, from equation (15)&(2), we would have two partial differential equations plus two mixed boundary equations (not pure Dirichlet or Neumann boundary conditions). The numerical solution of this is a rather complicated one.

An alternate approach which has been used in some papers [13] on LC was first suggested in Adler's paper on gauge field equilibrium equations [8]. The spirit of the method is direct differentiation. We use this method in our problem.

Reducing the Continuous Total Free Energy into Discrete Form

We first introduce a two-dimensional (ρ-z) computational square lattice, replace the continuous variables ρ and z by discrete ones, and rewrite the free energy in this discrete coordinate system. Due to symmetry we can limit the region of our study to a single quadrant of a circle. There are three kinds of unit cells (Fig. 5), corresponding to the three kinds of terms in the bulk free energy density. We use the corresponding unit cell in summing that term to get the total free energy.

An h-factor is assigned to each mesh point to take account of the boundary. Briefly speaking, h-factors of mesh points outside or inside boundary are 0 or 1, respectively; h-

factors of mesh points near the boundary are 1/2 or 1/4 according to their location on boundary. Each mesh point is associated with a unit cell, whose area is weighted by the h-factor: the h-factor will make some unit cells near boundary have half or one-fourth the area of a square.

TABLE 1. Reducing the continuum total free energy term to discrete form.

Continuum Term	Unit Cell	Discrete Form
$\int d\rho dz(\partial f/\partial \rho)^2$	Fig.5(a)	$\sum\sum \Delta\rho\Delta z h1_{i,j}(f_{i+1,j}-f_{i,j})^2/(\Delta\rho)^2$
$\int d\rho dz(\partial f/\partial z)^2$	Fig.5(b)	$\sum\sum \Delta\rho\Delta z h4_{i,j}(f_{i,j+1}-f_{i,j})^2/(\Delta z)^2$
$\int d\rho dz\ f$	Fig.5(c)	$\sum\sum \Delta\rho\Delta z h0_{i,j} f_{i,j}$

The definition of h-factor is as follows,

$$h1_{i,j}=\frac{1}{2}[h(i+1/2,j+1/2)+h(i+1/2,j-1/2)] \tag{17}$$

$$h4_{i,j}=\frac{1}{2}[h(i+1/2,j+1/2)+h(i-1/2,j+1/2)] \tag{18}$$

where h(x,y)=0 if (x,y) is outside the quadrant region; h(x,y)=1 if (x,y) is within the region.

Differentiation of the Total Free Energy

The condition for a stable configuration of the droplet is that the partial derivatives

of the total free energy with respect to each local variable S_{ij} and θ_{ij} vanish. For a given mesh point (i,j), the differentiation gives an equation for variable S_{ij} and an equation for variable θ_{ij}. The difference of formulations for each above equation, between bulk mesh points and surface mesh points, is only that the latter has the surface energy term added, as well as the same bulk term as the former.

Solving for S_{ij} and θ_{ij}

To find the roots of the above equations for given S_{ij} or θ_{ij}, we use Newton's method. Newton's iterative method for finding the roots of the equation f(x)=0 can be written as:

$$x^{(n+1)} = x^{(n)} - f(x^{(n)})/f'(x^{(n)}) \tag{19}$$

We use a variant of the basic method, called the successively over-relaxed (SOR) Gauss-Seidel iteration:

$$x^{(n+1),SOR} = \omega x^{(n+1)} + (1-\omega)x^{(n)} \tag{20}$$

where $0<\omega<2$, and the optimal value of ω is about 1 for the initial several iterations and about 1.8 for later iterations.

Now we can sweep the mesh. At every node, we execute a single iteration to update S_{ij} and θ_{ij}. During the iteration, we always use the most recent values of S and θ for nearby points. One sweep after another, we sweep until the difference between new values and old values are all less than some chosen criterion, --- that is, until convergence.

More Comment on the Boundary

As mentioned, in this method we need not specify or fix values of variables on the

boundary. The boundary points are iterated in almost the same manner as bulk points. Some considerations of symmetry can enable us to use fixed boundary values on some sides. This can both reduce the work and eliminate unwanted metastable configurations without symmetry. On the two sides of the quadrant, the ρ axis and the z axis, θ is equal to zero for bipolar structures and so we fix the value of θ on these sides.

Inclusion of the Shape Parameter

There is one parameter describing prolateness. For a given prolateness, we solve the stable configuration and calculate the total free energy, the plot of which vs. prolateness determines the shape parameter giving the minimum energy. Our trick to take account of the shape is as follows. For a sphere the unit cell of the lattice is taken to be a square, and for a prolate ellipsoid it is a rectangle. As Fig.(6) shows, we deform the sphere by a factor of x (shrinking the lateral and extending the vertical dimension), while conserving the volume of the droplet. At the same time, we also deform lattice by the same factor x. So, those mesh points outside droplet before deforming are outside after deforming, and the inside points remain inside. Thus the additional complexity of our program due to introducing prolate shapes is very limited.

Features of the Numerical Method

We summarize the advantages of our method as follows:

(1) Surface mesh points and internal points are iterated at the same sweep. Variables on surface need not be fixed.

(2) The method desplays fast convergence. For 40x40 mesh, 100 sweeps can make $|S_{new}-S|$ and $|\theta_{new}-\theta| < 10^{-6}$.

(3) The method is easily extended to additional problems. Due to the above two features, it is not difficult to approach problems with more complicated configurations such as might arise in taking account of three elastic constants.

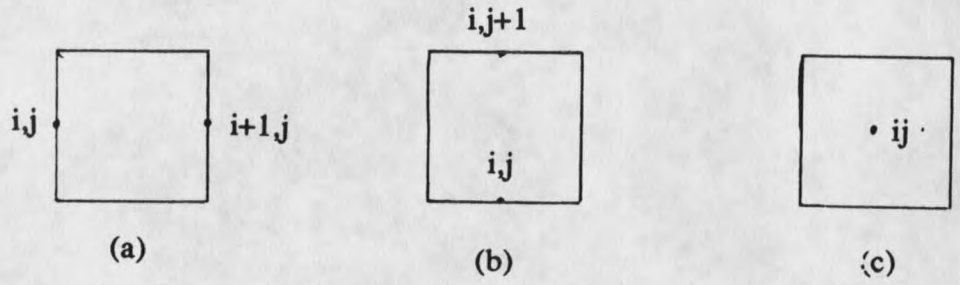

Figure 5. The unit cells for covering.

Darkened circles denote points of the computational lattice.

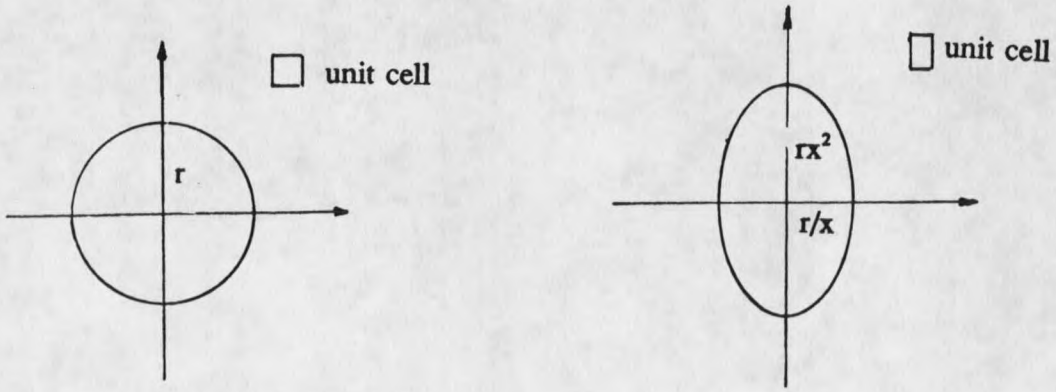

Figure 6. Shape Parameter x.

CHAPTER 4

RESULTS AND PHYSICAL EXPLANATION

The bulk coefficients a, B, C, and L_1 we used are of the nematic LC 5CB. $a=0.13J/cm^3K$, $B=1.605J/cm^3$, $C=3.9J/cm^3$, $L_1=10^{-13}J/cm$. The corresponding bulk supercooling limit $T^*=317.14K$ is 1.129K below the bulk nematic-isotropic transition temperature. $T-T_c^*$ is set at 0.001°. We focus on tangential anchoring. When we study structure, in section (A) and (B), we fix the shape as a sphere. This is practical if the environment is solid like PDLC or if prolateness is negligible.

Director Field

We find the interesting result that the configuration of the director field shows a transition from nondistorted (or less distorted) to distorted as either r or w_0 varies (Fig.12 & 14). "Distorted" means there is significant variance of $\mathbf{n}$ in the droplet, which can be described by θ_{max}. The exception is that for anchoring strength greater than $0.02J/m^2$, the configuration remains constantly highly distorted with respect to r, i.e. no transition, and for radius greater than 1000μm, the configuration remains constantly highly distorted with respect to w_0. The transition with respect to w_0 can become very abrupt for small droplets and in that case we recognize the transition as a first-order one.

One result drawn from above is that for large droplet, there is always effectively strong anchoring, even if the anchoring strength parameter is small. This is confirmed by an analytical approach due to Williams [7] and experimental photographs [12].

The decrease in the degree of distortion when the droplet becomes smaller is understandable on the basis of our previous dimensional analysis which showed that, for smaller droplets, the bulk term becomes more and more dominant, in the competition with the surface anchoring which tends to cause distortion. In other words, the function of reducing size is almost equivalent of that of reducing w_0.

Our results showing nondistorted configurations have not been reported before, but are physically reasonable and expected. As droplet becomes too small or anchoring strength is too weak, the bending energy of a distorted configuration will become relatively large, compared with the anchoring energy. So the configuration is not distorted at all. Another interesting way to see this result is that, the LC molecules are about several tens of Angstroms long, so for a droplet about several hundreds Angstroms big, it is really impractical for the molecules to align along the surface direction since such configuration is hardly an efficient packing.

Order Parameter

Somewhat more complex but no less interesting results are obtained for the order parameter S. (FIG 9, 10, 11, and 13)

For large w_0, (e.g. $>0.001 J/m^2$), the configuration of the S field shows two transitions from distorted to nondistorted as r varies. For small r, S is uniformly zero, while for large r S is uniform at the bulk sample value; in between the S field is non-uniform. For small w_0, S takes on the uniform bulk value no matter what the size of the droplet. (Fig. 9, 10 and 11)

For big w_0, the maximum value of S over the droplet has a discontinuous transition from zero to the bulk value as r increases. The transition point corresponds to the point A of Fig.10.

For a small droplet a point defect of the S field (shown from the near vanishing of S_{min}) appears abruptly as w_0 varies. For a large droplet, S is always the uniform bulk value as w_0 varies (Fig.13). The variation of S_{min} with respect to r is also from zero to bulk value but not as abrupt as maximum S. (Fig. 9)

The above results are reasonable. The phenomenon of uniformly zero S for small droplets and strong anchoring is especially interesting, since this is an order/disorder phase transition induced by size and not by temperature. There is a clear physical picture of this result. We note from the Fig.14 that, for strong anchoring, the director field is distorted with constant configuration as r varies. So for a small enough droplet, such

distortion is serious enough to destroy the ordering of molecules. We can also understand this by looking at the equation (14), in which there are two terms containing S^2: one is related to temperature and the other to the distortion of the director field. So it is very natural that some factors other than temperature can also induce order/disorder phase transition, due to the second term.

The data of our figures is obtained at a temperature below but near T_c. We have tried other temperatures below T_c, and find that the above kind of order/disorder transition still exist.

We notice that r can induce both a distortion/ nondistortion transition and an order/disorder transition, but w_0 can only induce a distortion/ nondistortion transition. This conforms to our above explanation of the reason for the order/disorder transition.

Comparing Fig.12 and Fig.13, we find that the point of the distortion/ nondistortion phase transition of the S field agrees with the point of the distortion/ nondistortion transition of the **n** field. This explains the reason for the distortion of the S field --- namely, due to the coupling between S and **n**. The more serious the bending of the **n** field, the smaller the order parameter. Fig.15 is a picture of the S field, with gray-scale density representing the magnitude of S. We can see vividly the above relationship between S and **n**.

Shape

Our computational results show that the change of the bulk energy with shape cannot compete with that of the surface energy, no matter how extraordinarily we manipulate the bulk and surface coefficients. For a large droplet, the absolute value of the bulk energy can be several orders of magnitude bigger than that of the surface energy, but the surface energy still dominates in the problem of shape. The physical explanation makes this result understandable. With a small change of shape, the change of bulk energy, ΔF_b, is proportional to the bulk coefficients and the degree of distortion of the director field. If the bulk coefficients increase, the distortion decreases due to the competition of bulk and surface energies in getting the stable configuration, and so ΔF_b increases little, if any. If we increase the surface anchoring strength w_0 to increase the distortion, then the bulk energy increases; but since the surface tension constant σ must be greater than w_0 (w_0 is a perturbation of σ), then the surface energy also increases.

Surface term itself can make the prolate shape appear. As Fig. 8 shows, a large droplet is spherical; as the size becomes smaller, the droplet becomes more elongated and approaches a constant prolateness, which is maintained nicely as the radius approaches zero. The limiting prolateness (quantity x-1 at $r \rightarrow 0$) for a given size droplet is almost proportional to w_0/σ (Fig.7).

The understanding of the above prolateness results relies on our previously acquired knowledge of the the structure. Now that we know the shape is only determined by the

surface term, only the degree of distortion of the **n** field contributes to the shape, besides w_0 and σ. As we remarked above, for a large droplet there is always effectively strong anchoring, so the director at the surface is perfectly tangential to the surface. Therefore, the surface energy density (2) is a constant and the spherical shape, which has minimum area, is stable. As the droplet becomes smaller, the distortion decreases and the director at the surface is not perfectly tangential. The elongated shape will decrease the angle between **n** and α over most of the surface, and so decrease the surface energy. As the **n** field becomes uniform, the prolateness achieves its maximum, which is maintained for the even smaller droplet since its **n** field remains uniform.

The relationship between the limiting shape and the ratio w_0/σ is easily understood from equation (2). We already know the **n** field of the droplet having the maximum degree of prolateness and different w_0 is the same, i.e., uniform, so from equation (2) only w_0/σ plays a role in influencing shape. And since x-1 is small, the nearly linear relationship is expected.

Normal Anchoring

A change of a few statements in our program gives configurations for the normal anchoring condition, which has results similar to those above. Fig.16 shows the S field of the axial configuration.

Reliability of Results

We tried a denser mesh (400x400), and found that the final state configurations did

not change. We also tried different initial values of the S field and **n** fields, and in most cases we get the same final states, which is quite marvelous since relaxation can only guarantee that the final convergent state is one of the metastable states.

We used approximations of one-elastic-constant and no twist. If we take account of 3 elastic constants and twist, we will generate the twisted-bipolar configuration. But from our preceding physical explanation, the essential features of our results should still hold.

On the Temperature Induced Phase Transition

In a separate paper [14], using the same computer program as this work, we show how temperature induces order/disorder transitions for LC droplet. Our theoretical results explain the experimental paper [15], but have very different mechanism from the theoretical paper [5] on the same subject. Briefly speaking, the deuterium NMR experiment showed that small tangentially anchored LC droplets (less than 0.035μm in diameter) show a certain degree of order at temperature above T_c and the nematic/isotropic (N-I) transition is a continual evolution rather than first-order in the case of large droplet. The theoretical computational calculation assumed strong anchoring condition (i.e. strong distortion of the **n** field) for droplets of all sizes and assumed fixed large S value on surface, and then showed results agreeing with experiment, in which the remaining order at high temperature comes from the layer near surface. Our results show the configurations of **n** are uniform for small droplets, which cause the non-vanishing

order above T_c. From the previous physical interpretation it seems our results are more sensible physically.

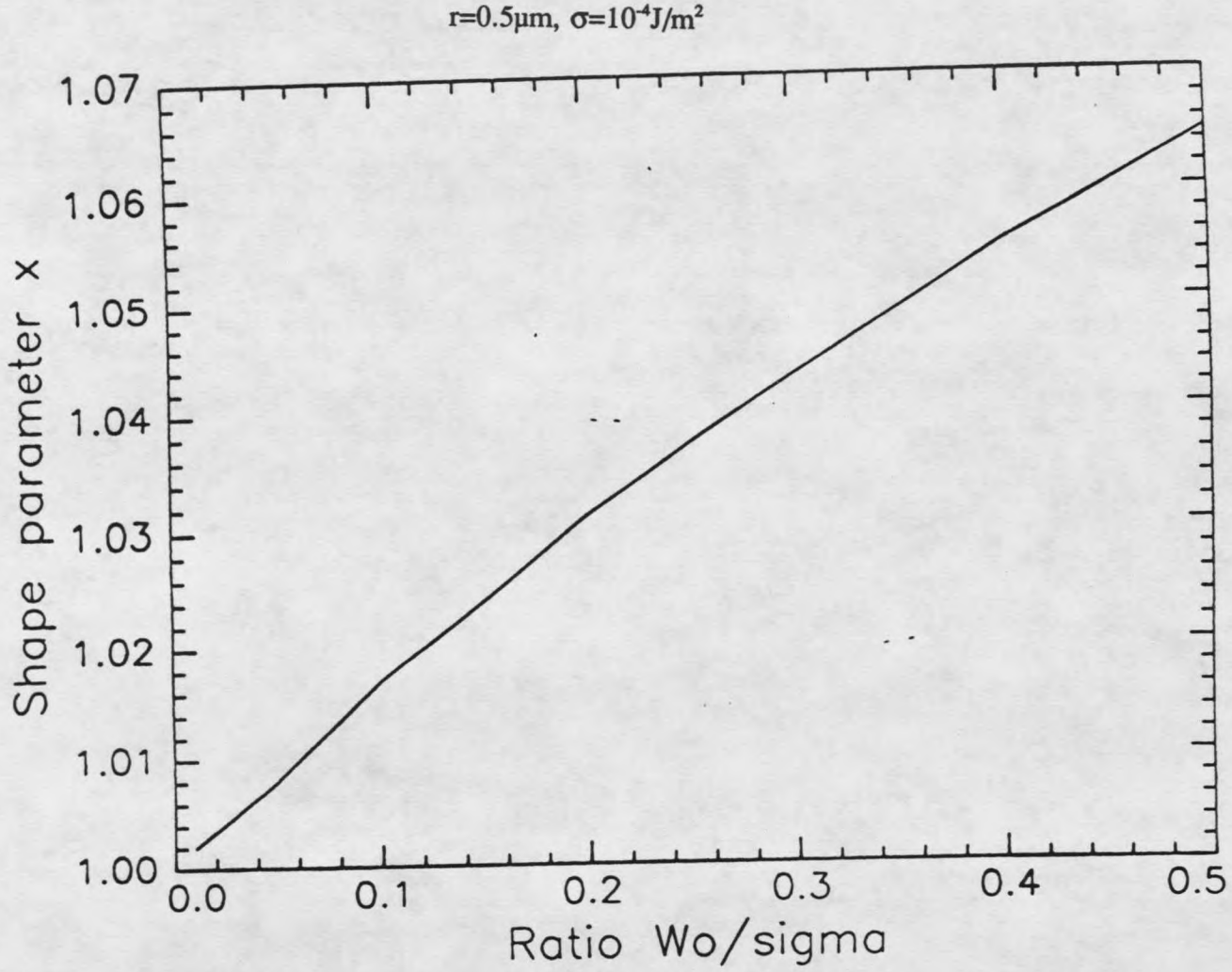

Figure 7. Curve x-$w_{0/\sigma}$

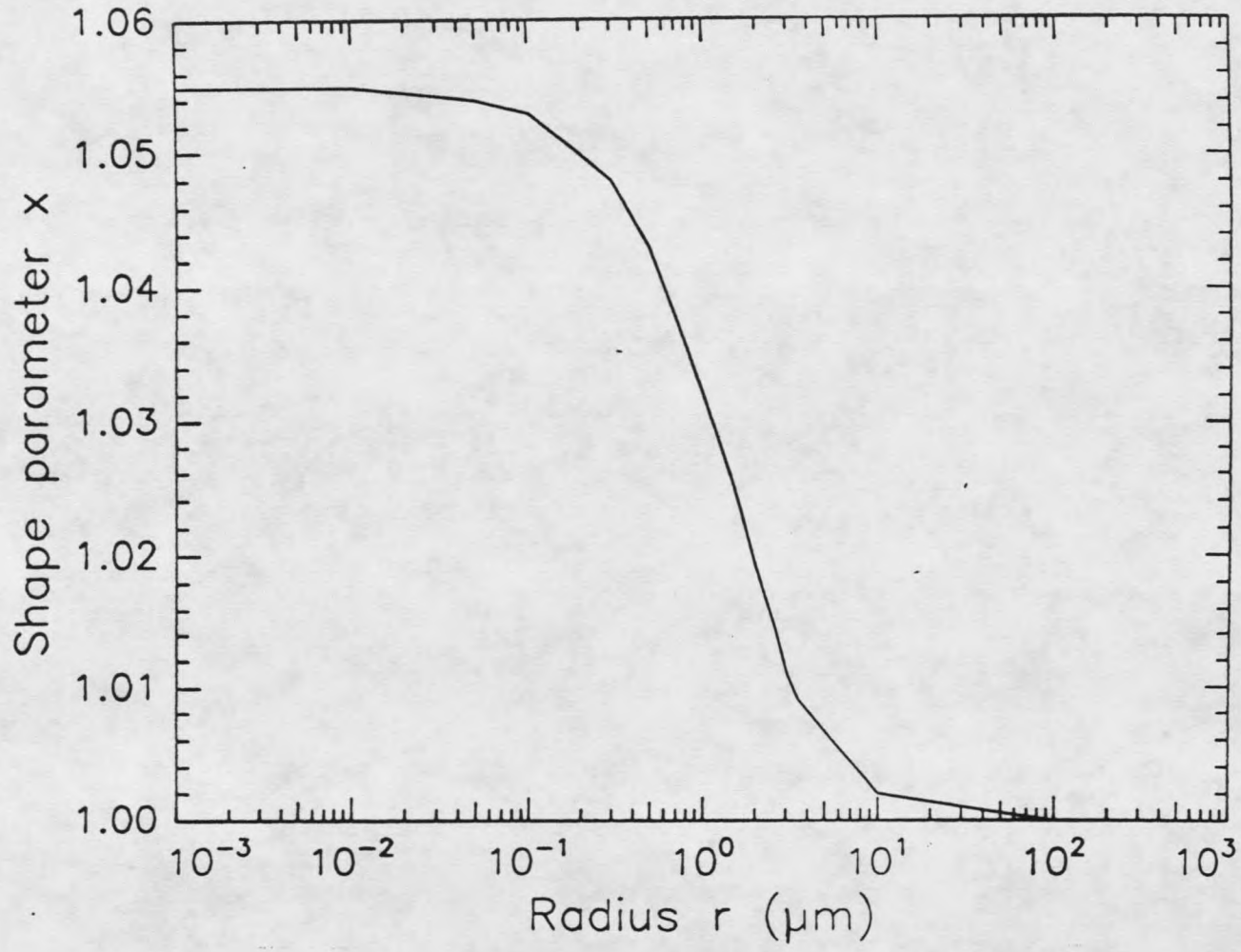

Figure 8. Curve x-r

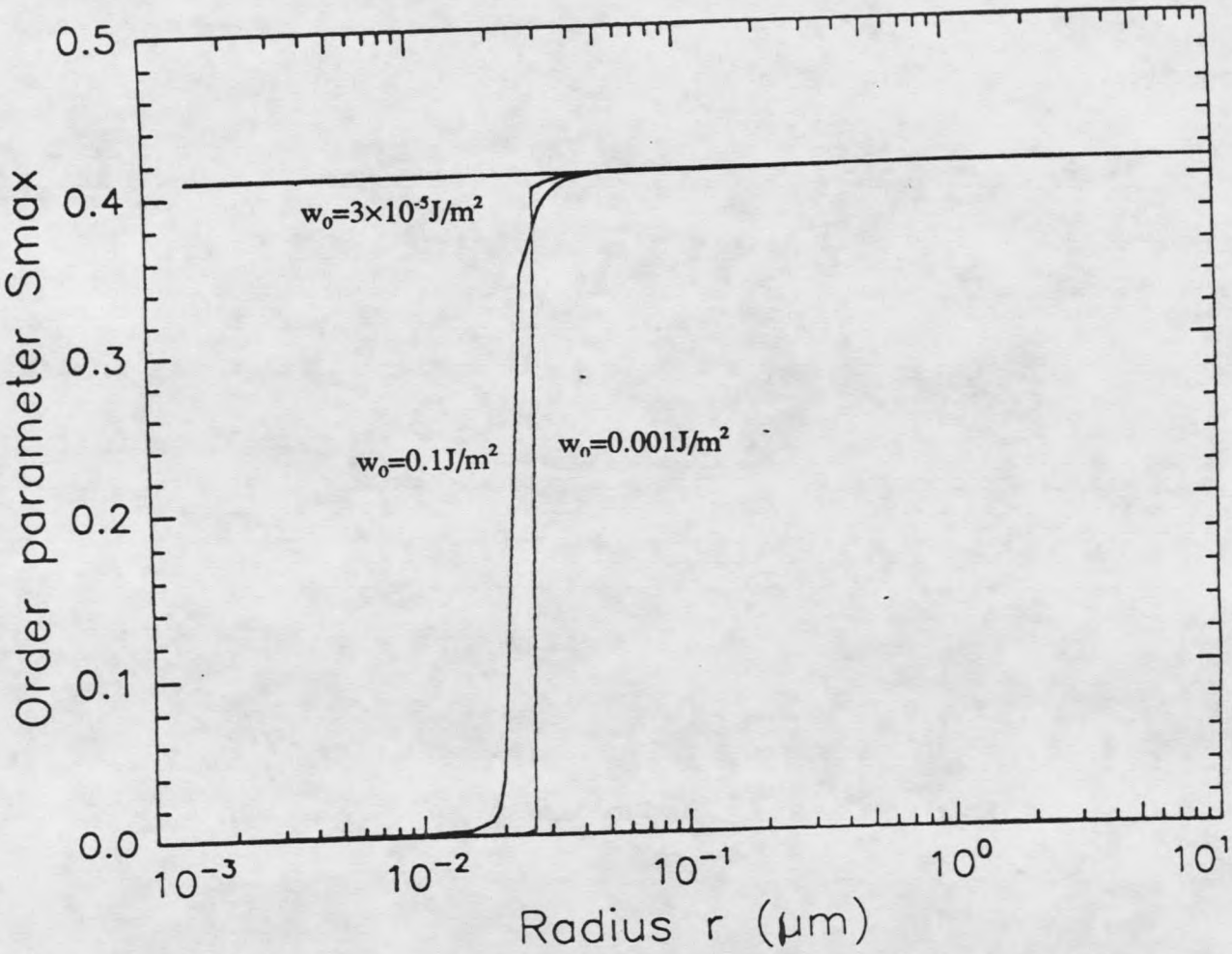

Figure 9. Curve S_{max}-r

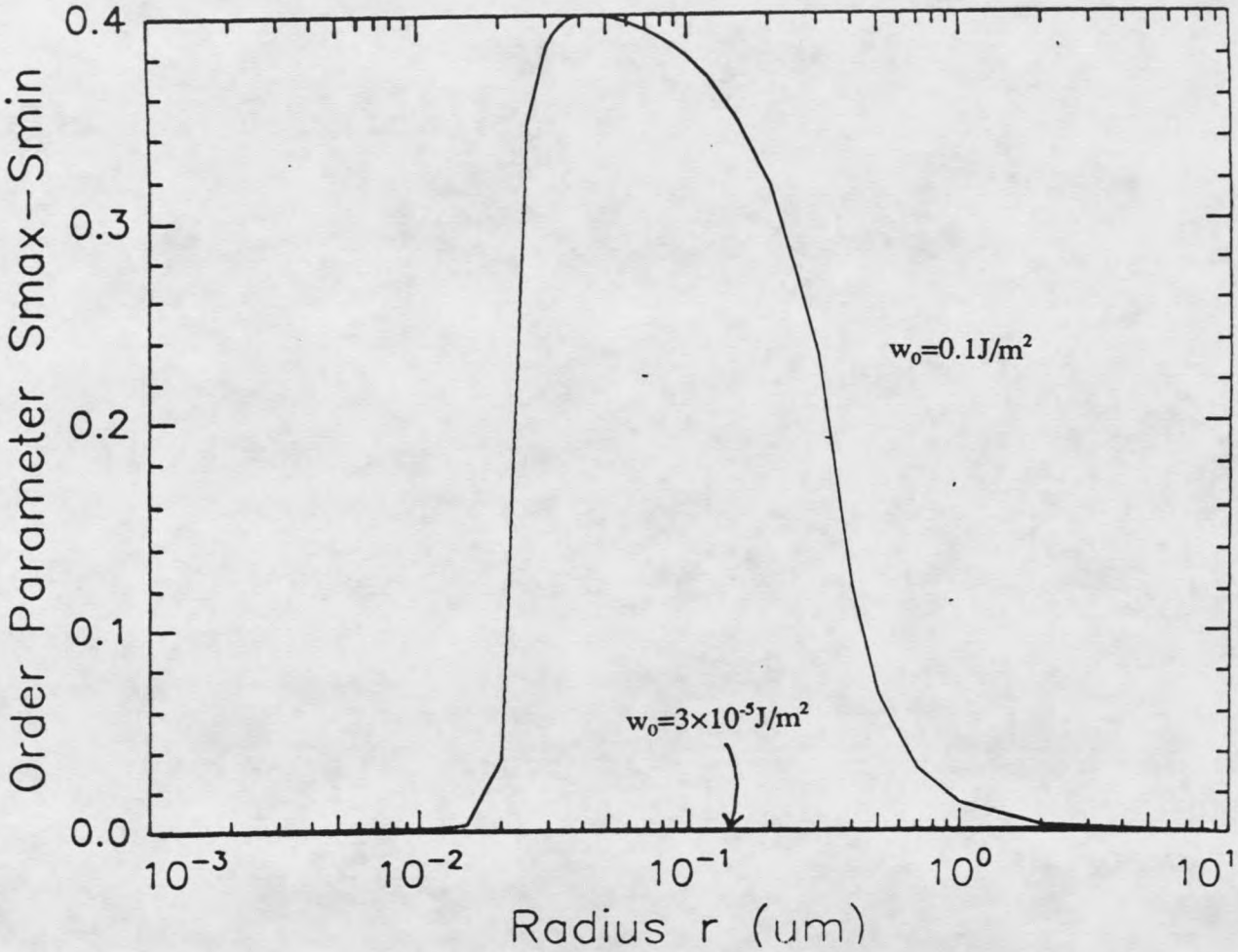

Figure 10. Curve (S_{max}-S_{min})-r

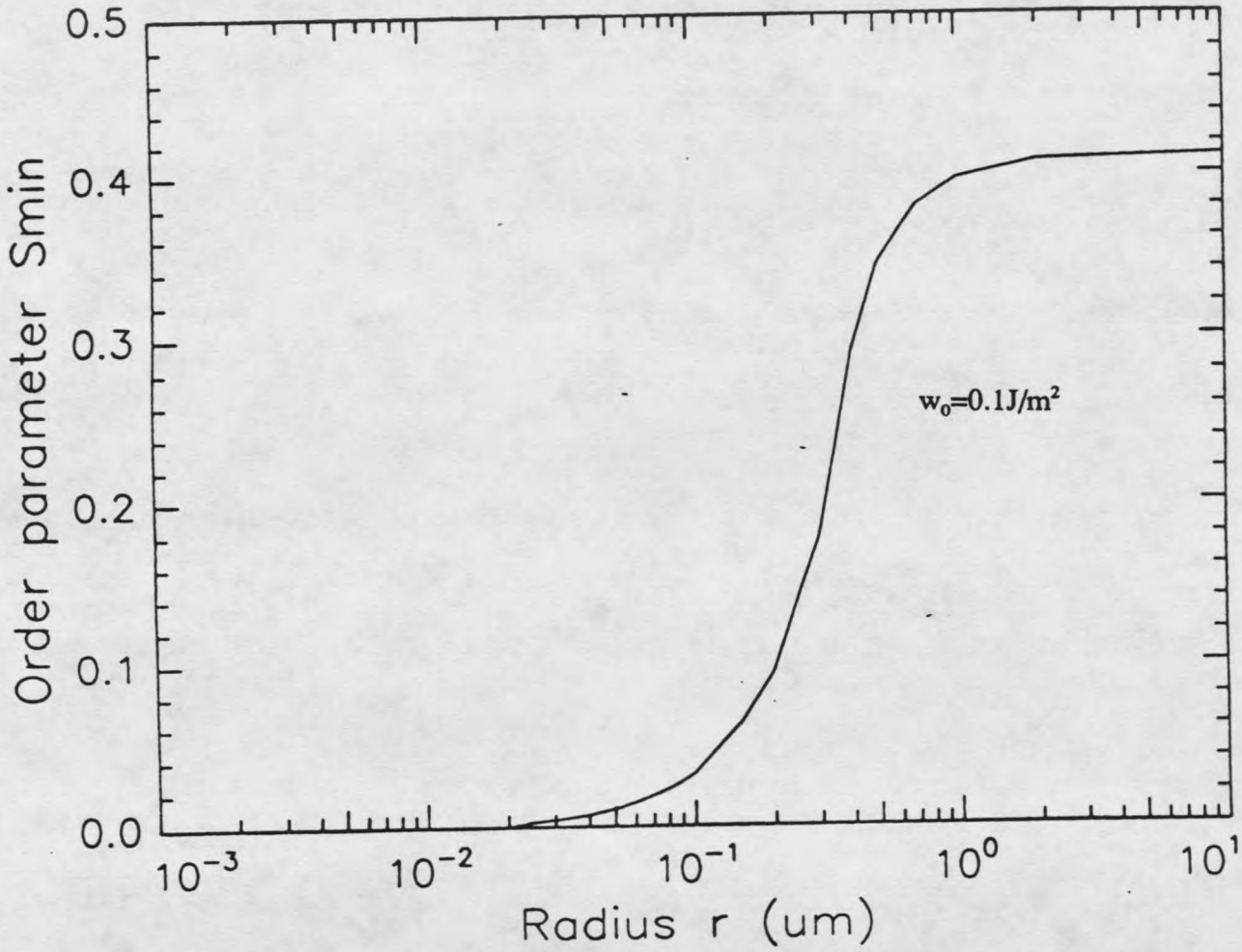

Figure 11. Curve S_{min}-r

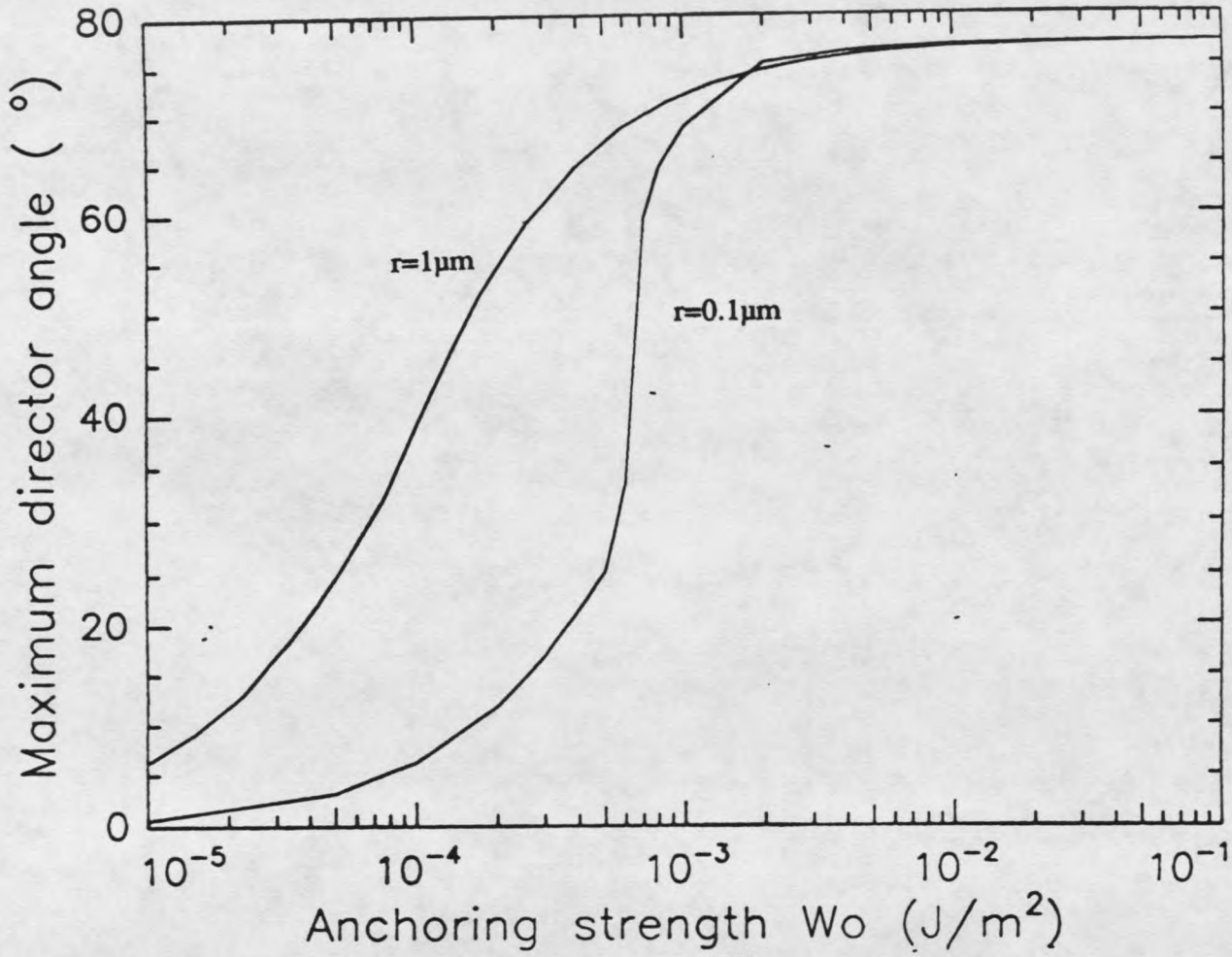

Figure 12. Curve θ_{max}-w_0

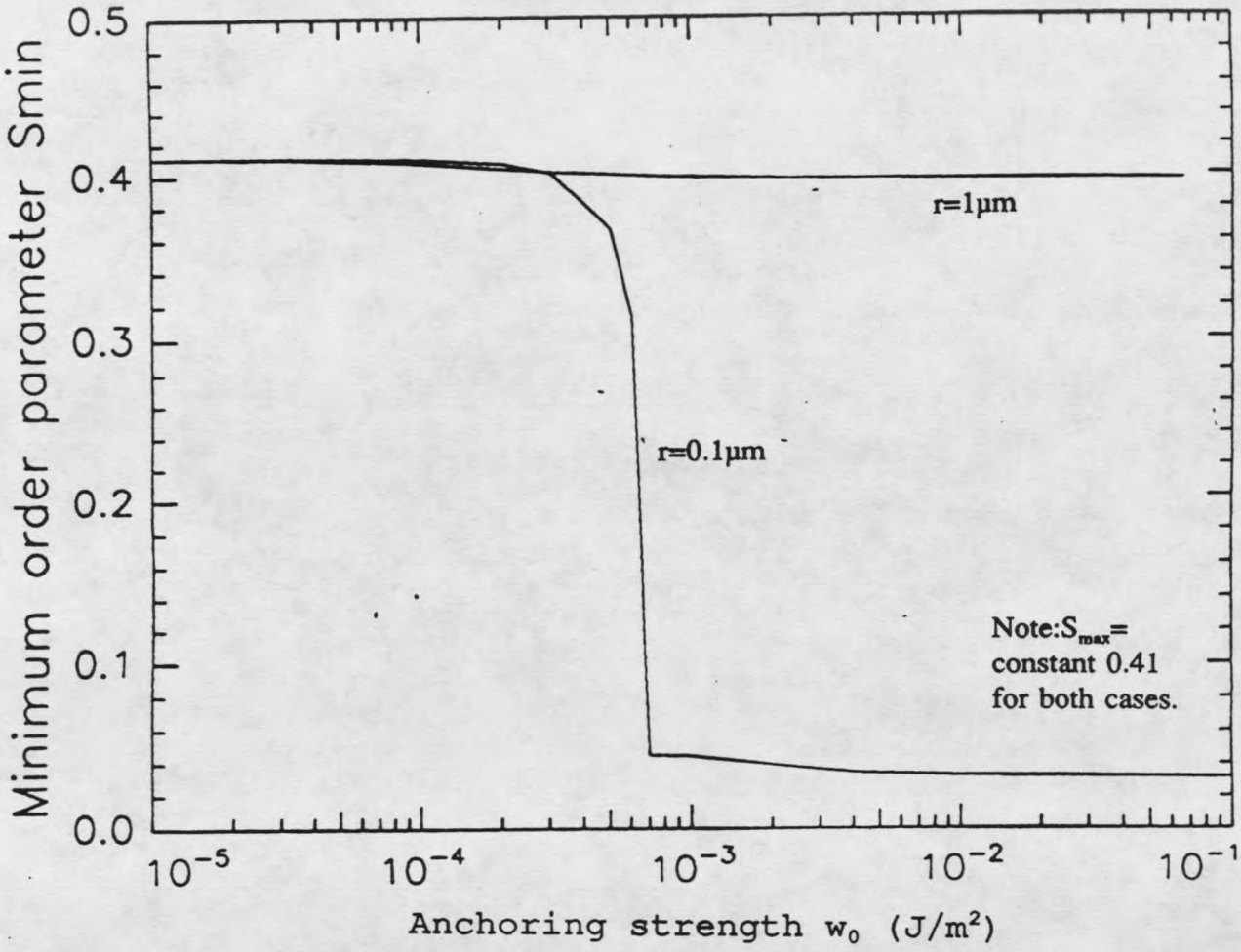

Figure 13. Curve S_{min}-w_0

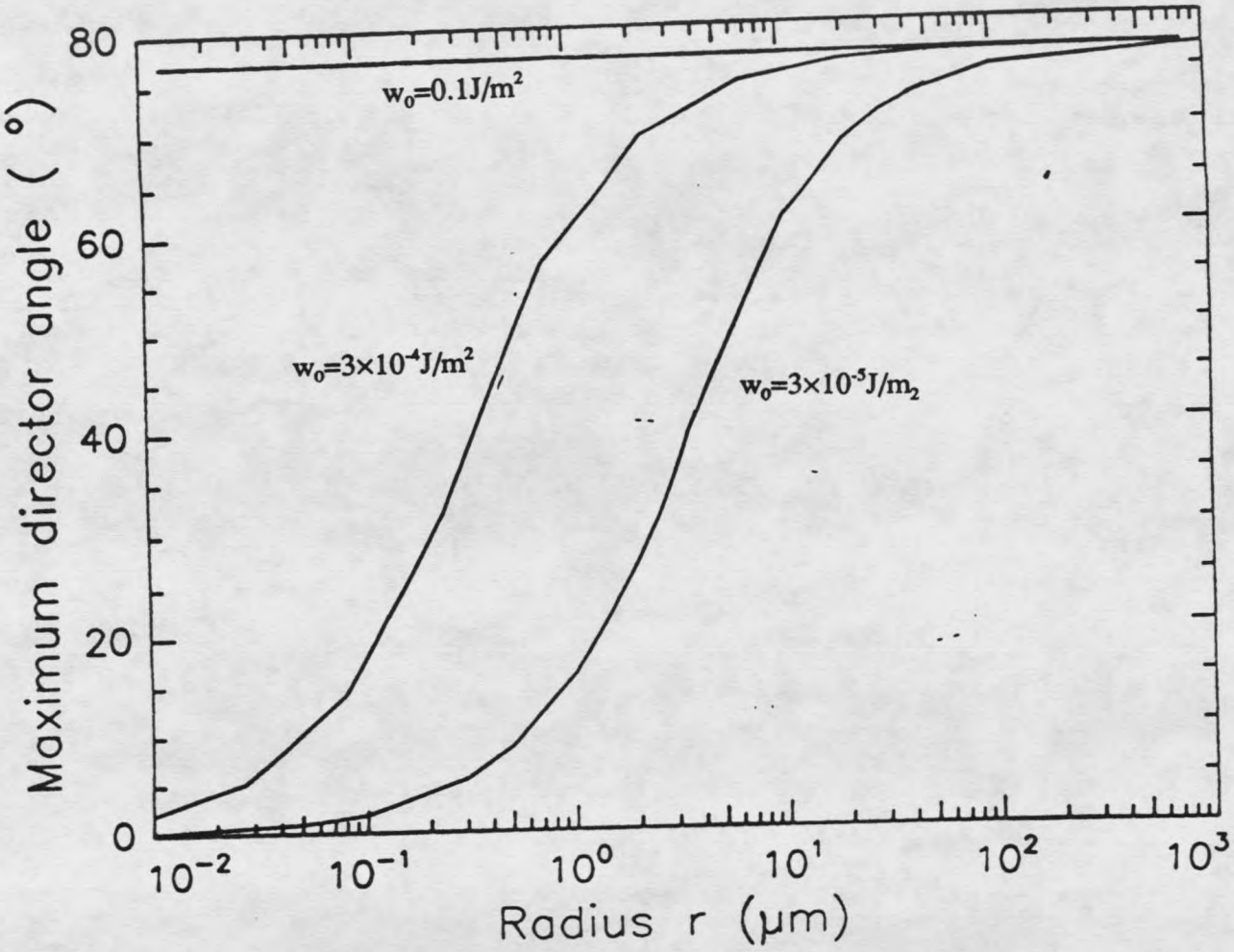

Figure 14. Curve θ_{max}-r

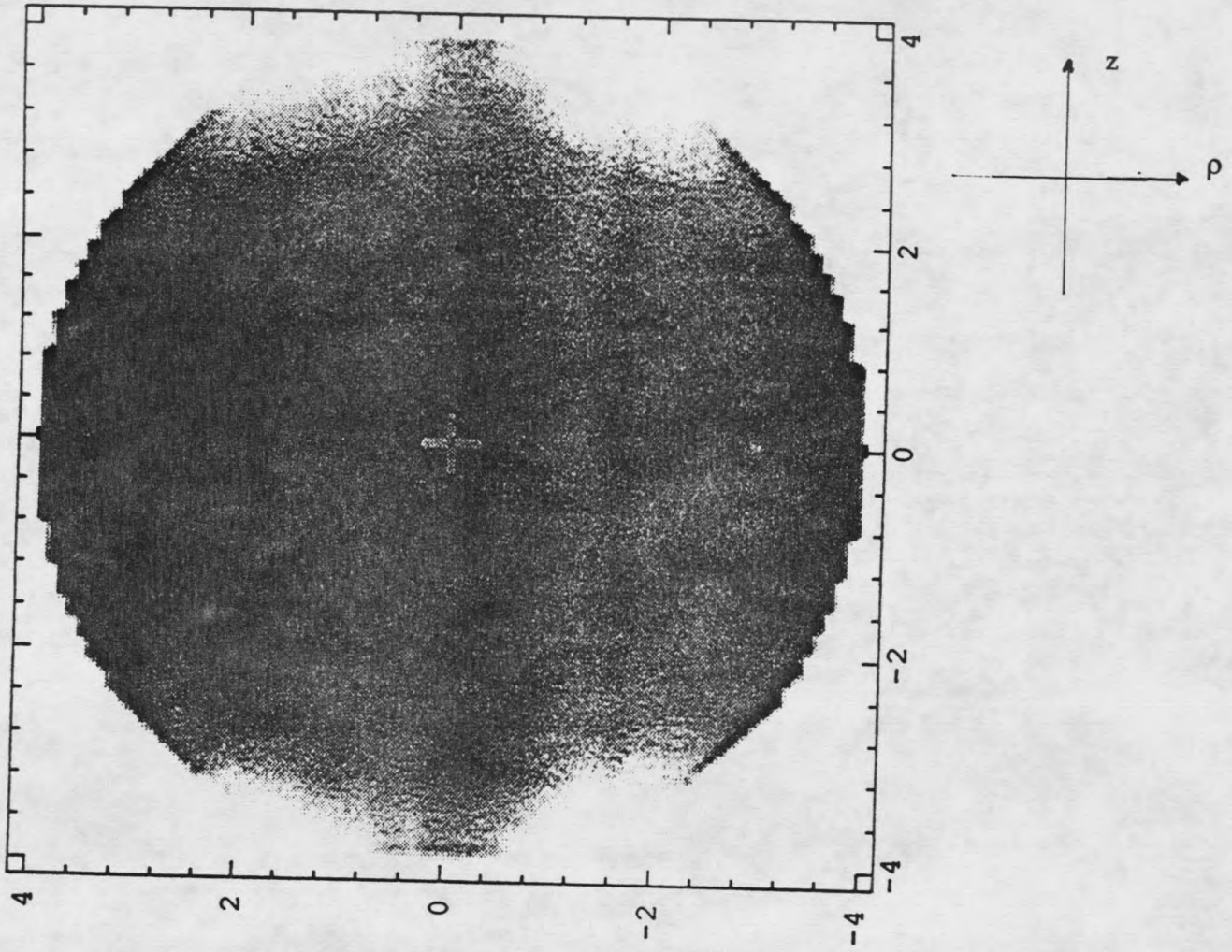

Figure 15. Graph of S field for tangentially anchoring condition.

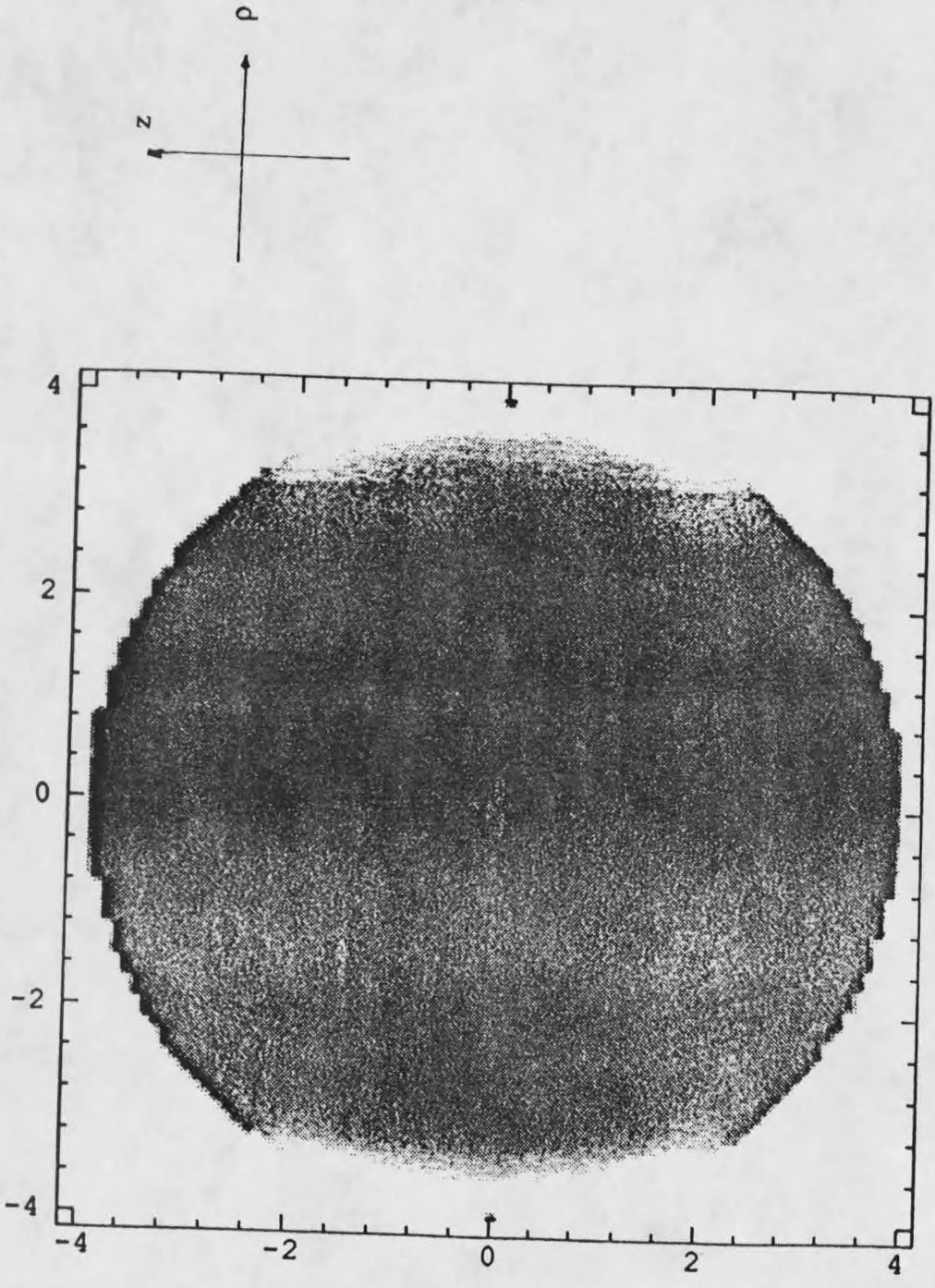

Figure 16. Graph of S field for normal anchoring condition.

CHAPTER 5

SUMMARY OF CONCLUSIONS

In the above theoretical studies we have developed a complete picture of the continuous dependencies of LC microdroplet structure and shape on several parameters, primarily anchoring strength and size, and we show some interesting structural phase transition predictions. These include a distortion/uniform transition of the S and **n** fields, an order/disorder transition, and a sphere/prolate ellipsoid transition. Some of these transitions appear to resemble first order phase transitions, in that they involve discontinuous changes of the configurations.

Droplets of small size (typically less than 1μm in diameter) or weak surface anchoring will have uniform or less distorted **n**. Under strong anchoring, small size can induce the N-I transition of LC droplet. Distortion of the S field appears abruptly as w_0 increases. Small sized free LC droplets have prolate shapes whose prolateness increases as w_0/σ increases but is not influenced by bulk coefficients.

This work gives us more understanding of LC microdroplets, which are useful in applications. The predictions made can be tested by experiment such as NMR, SEM, etc. The further continuation of this work may be in taking account of three elastic constants and twist and/or external field in studying LC droplets or capillaries.

REFERENCES

[1] W.Doane, N.Vaz, B.Wu, and S.Zumer, Appl.Phys.Letts. **48**,269 (1986)

[2] E.Dubois-Violette and O.Parodi, J.Phys.C 4,57 (1969)

[3] P.Drzaic, Mol.Cryst.Liq.Cryst. **154**,289 (1988)

[4] S.Kralj, S.Zumer, and D.Allender, Phys.Rev.A **43** 2943 (1991)

[5] I.Vilfan, M.Vilfan, and S.Zumer, Phys.Rev.A **40** 4724 (1989)

[6] S.Kralj and S.Zumer, Phys.Rev.A **45**, 2461 (1992)

[7] R.D.Williams, J.Phys. A **19**,3211 (1986)

[8] S.Adler and T.Piran, Rev.Mod.Phys., Vol. 56, No.1 (1984)

[9] J.Erdmann, S.Zumer, and J. Doane, Phys.Rev.Letts **64**, 1907 (1990)

[10] A.Golemme, S.Zumer, J.Doane, and M.Neubert, Phys.Rev.A **37**, 559 (1988)

[11] G.Vertogen and W.deJeu, "Thermotropic Liquid Crystals, Fundamentals", Chapter 9, Springer -Verlag(Berlin), (1988)

[12] Ondris-Crawford, J.Appl.Phys.,Vol.69, No.9; 6381 (1991)

[13] I.Vilfan, M.Vilfan, and S.Zumer, Phys.Rev.A **43** 6875 (1991)

[14] W.Huang & G.Tuthill, in process.

[15] A.Golemme, S.Zumer, D.Allender, and J.Doane, Phys.Rev.Lett. **61**, 2937 (1988)

APPENDIX

Computer Program with FORTRAN Language

Figure 17. FORTRAN computer program for the main work.

```
      implicit real*4 (a-h,o-z)
      real a(-1:41,-1:41), s(-1:41,-1:41), h1(-1:41,-1:41),
     c  h4(-1:41,-1:41), h0(-1:41,-1:41), hne(-1:41,-1:41),
     c  hse(-1:41,-1:41), hsw(-1:41,-1:41), hnw(-1:41,-1:41), p(-1:41),
     c  s2(-1:41,-1:41),sin2a(-1:41,-1:41),
     c  sina2(-1:41,-1:41), cos2a (-1:41,-1:41)

*     Notation: "a" for theta, "s" for S, "h1"-"hnw" are h-factors, "p" for
*       rho, "s2" for the square of S, "sin2a" for sin(2*a), "sina2"
*       for sin(a)**2, "cos2a" for cos(2*a).

      open(9,file='v8.dat',status='new')

      Aaa=1.3E5
      td=0.001
      a2=aaa*Td/2.
      b=1.605E6
      a3=-B/3.
      c=3.9E6
      a4=c/4.
      qq1=1.0E-11
      a1=0.75*qq1
      a6=2.25*qq1
      radius=500.E-10
      sigma=1.0E-4
      w=1.
      w0=1000.*sigma

*     Notation: "aaa" - "a6" are bulk coefficients, "w" is the over relaxation
*               constant.

*     The following loop is to set initial values of S and n, and define
*        h-factors.

      do 1 j=0,41
      do 2 i=0,41

      if (i**2+j**2 .gt.1600)goto 3
      s(i,j)=1.0
```

```
      a(i,-1)=0.
      a(-1,j)=0.
      a(i,0)=0.
      a(0,j)=0.
      a(i,1)=0.
      a(1,j)=0.
      s2(i,j)=s(i,j)**2
      sin2a(i,j)=sin(2*a(i,j))
      cos2a(i,j)=cos(2*a(i,j))
      sina2(i,j)=sin(a(i,j))**2


      if ((i+0.5)**2 +(J+0.5)**2 .gt. 1600.) goto 70
      hne(i,j)=1.
      goto 71
70    hne(i,j)=0.
71    If (j.eq.0) goto 72
      hse(i,j)=1.
      goto 73
72    hse(i,j)=0.
73    if (i.eq.0 .or.j.eq.0) goto 74
      hsw(i,j)=1.
      goto 75
74    hsw(i,j)=0.
75    if (i.eq.0) goto 76
      hnw(i,j)=1.
      goto 77
76    hnw(i,j)=0.
77    h1(i,j)=(hne(i,j)+hse(i,j))/2
      H1(-1,j)=0
      h4(i,j)=(hnw(i,j)+hne(i,j))/2
      h4(i,-1)=0
      h0(i,j)=(hne(i,j)+hse(i,j)+hsw(i,j)+hnw(i,j))/4
      goto 2
3     a(i,j)=0.
      s(i,j)=0.
      sina2(i,j)=0.
      sin2a(i,j)=0.
      cos2a(i,j)=0.
      s2(i,j)=0.

2     continue
1     continue
```

```
      x=1.
      remf=1.

*     "remf", "rema", and "rems" are to remember old values of f, a, and S,
*          respectively.
*     The following loop is one sweep over the quadrant.

99    coma=0.
      coms=0.

*     "coma" and "coms" denote the largest absolute values of the differences
*          between new theta and old theta or new S and old S of any node
*          in the quadrant,

      dp=radius/40./x
      dz=radius/40.*x**2
      fs=sigma*dz*6.2832*radius*2./x
      isur=0
      jsur=40

*     "dp" and "dz" are length of unit cell along rho and z axis, repectively.
*          "fs" denote the total surface free energy. "isur" and "jsur" are
*          for the use of summing up surface energy.

      do 10 j=40,1,-1
      do 20 i=40,1,-1

      if(i**2+j**2 .gt.1600) goto 20
      if((i+1)**2+j**2 .le.1600 .and. i**2+(j+1)**2.le.1600)
     a goto 55
      if((i+1)**2+j**2 .gt.1600 ) h1(i,j)=0.
      if(i**2+(j+1)**2 .gt.1600 ) h4(i,j)=0.

55    p(i)=radius/40.*(i+0.001)/x
      p(0)=radius/40.*0.001/x
      p(40)=radius/x
      rema=a(i,j)
      rems=s(i,j)

      s(i,0)=s(i,1)
      s(0,j)=s(1,j)
      s2(i,0)=s(i,0)**2
      s2(0,j)=s(0,j)**2
```

```
      q1=( a(i,j)-a(i+1,j) )
      q2=( a(i,j)-a(i-1,j) )
      q3=( a(i,j)-a(i,j+1) )
      q4=( a(i,j)-a(i,j-1) )
      qa=-q1
      qb=-q2
      qc=-q3
      qd=-q4


      G1=h0(i,j)*a6*s2(i,j)/p(i)*sin2a(i,j)
     a + h1(i,j)*a6*( p(i+1)*s2(i+1,j)+p(i)*s2(i,j) )
     a /dp**2*( q1 )
     a +h1(i-1,j)*a6*( p(i)*s2(i,j)+p(i-1)*s2(i-1,j) )
     a /dp**2*( q2 )

      g2=g1+h4(i,j)*a6*p(i)*( s2(i,j+1)+s2(i,j) )
     a /dz**2*( q3 )
     a +  h4(i,j-1)*a6*p(i)*( s2(i,j)+s2(i,j-1) )
     a /dz**2*( q4 )
     a +      h1(i,j)*a6/2/dp*(  s2(i,j)*2*cos2a(i,j)
     a *( qa )-sin2a(i+1,j)*s2(i+1,j)
     a -   sin2a(i,j)*s2(i,j)  )

      g3=g2+h1(i-1,j)*a6/2/dp*(  s2(i,j)*2*cos2a(i,j)
     a *( q2 )+   sin2a(i,j)*s2(i,j)
     a +sin2a(i-1,j)*s2(i-1,j)  )

      g4=g3+ h4(i,j)*a6/dz*(  s2(i,j)*sin2a(i,j)
     a *( qc )-sina2(i,j+1)*s2(i,j+1)
     a -   sina2(i,j)*s2(i,j)  )

      g=g4+h4(i,j-1)*a6/dz*(  s2(i,j)*sin2a(i,j)
     a *( q4 )+   sina2(i,j)*s2(i,j)
     a +sina2(i,j-1)*s2(i,j-1)  )

*     "G" denotes the derivative of total free energy with respect to theta
*        of a given node.

      gd1=h0(i,j)*a6*s2(i,j)/p(i)*2*cos2a(i,j)
     a + h1(i,j)*a6*( p(i+1)*s2(i+1,j)+p(i)*s2(i,j) )/dp**2
     a +h1(i-1,j)*a6*( p(i)*s2(i,j)+p(i-1)*s2(i-1,j) )/dp**2
     a + h4(i,j)*a6*p(i)*( s2(i,j+1)+s2(i,j) )/dz**2
     a +h4(i,j-1)*a6*p(i)*( s2(i,j-1)+s2(i,j) )/dz**2
```

```
      gd2=gd1
     a -h1(i,j)*a6/dp*s2(i,j)*(  2.* sin2a(i,j)
     a         *( qa )+cos2a(i,j)  )
     a -h1(i,j)*a6/dp*cos2a(i,j)*s2(i,j)
     a +h1(i-1,j)*a6/2./dp*          (
     a    -s2(i,j)*4.*sin2a(i,j)*q2
     a    +s2(i,j)*2.*cos2a(i,j)
     a    +2.*cos2a(i,j)*s2(i,j)     )

      gd=gd2
     a +h4(i,j)*a6/dz*               (
     a       s2(i,j)*2*cos2a(i,j)*qc
     a      -s2(i,j)*sin2a(i,j)
     a      -sin2a(i,j)*s2(i,j)      )
     a +h4(i,j-1)*a6/dz*             (
     a       s2(i,j)*2*cos2a(i,j)*q4
     a      +s2(i,j)*sin2a(i,j)
     a      +s2(i,j)*sin2a(i,j)      )

*     "gd" denotes the derivative of "G" with respect to the theta of a
*         given node.

*     The following paragragh is to get the "G" and "GD' for the surface mesh points

      if (j.lt.8)goto 66
      if((i+1)**2+j**2.le.1600)
     a goto 52
      goto 68
66    if (i.eq.39)goto 68
      goto 52
68    y=radius/40.*(j+0.001)*x**2
      dl=sqrt(((i-isur)*dp)**2+((j-jsur)*dz)**2)
      da=6.2832*p(i)*dl
      beta=atan(y/x**6/p(i))
      gs=0.5*da*w0*sin(2.*(a(i,j)-beta))
      g=g*12.56*dp*dz+gs
      gd=gd*12.56*dp*dz+da*w0*cos(2.*(a(i,j)-beta))
      isur=i
      jsur=j

  52  if (gd.eq.0.) goto 53

*     The following paragraph is to update theta with one step.
```

```
      aold=a(i,j)
      a(i,j)=amod((w*(a(i,j)-g/gd)+(1-w)*a(i,j)),6.2832)
      if(a(i,j).lt.-0.2.or.a(i,j).gt.2.)a(i,j)=aold

   53 sina2(i,j)=sin(a(i,j))**2
      sin2a(i,j)=sin(2*a(i,j))
      cos2a(i,j)=cos(2*a(i,j))
      if (i.eq.39 .and.j.lt.8) goto 81
      if ((i+1)**2+j**2 .le.1600)goto 80
81    fs=fs+da*(sigma-0.5*w0*(cos(a(i,j)-beta))**2)
   80 if(abs(a(i,j)-rema).lt.coma)goto 50
      coma=abs(a(i,j)-rema)
      ia=i
      ja=j
   50 continue

*     "ia" and "ja" are to remeber the point which has "coma".

      r1=h0(i,j)*p(i)*(  2*a2*s(i,j)+3*a3*s2(i,j)
     a +4*a4*s(i,j)*s2(i,j)  )
     a +  h1(i,j)*a1/dp**2*(s(i,j)-s(i+1,j))*(p(i)+p(i+1))
     a +h1(i-1,j)*a1/dp**2*(s(i,j)-s(i-1,j))*(p(i)+p(i-1))

      r2=r1
     a +  h4(i,j)*a1/dz**2*(s(i,j)-s(i,j+1))* 2*p(i)
     a +h4(i,j-1)*a1/dz**2*(s(i,j)-s(i,j-1))* 2*p(i)
     a +h0(i,j)*a6*sina2(i,j)/p(i)*2*s(i,j)

      r3=r2+h1(i,j)*a6*( qa )**2/dp**2
     a *p(i)*s(i,j)
     a +   h1(i-1,j)*a6*( q2 )**2/dp**2
     a *p(i)*s(i,j)
     a +  h4(i,j)*a6*( qc )**2/dz**2*p(i)*s(i,j)
     a +h4(i,j-1)*a6*( q4 )**2/dz**2*p(i)*s(i,j)

      r=r3+h1(i,j)*a6*s(i,j)*sin2a(i,j)*( qa )/dp
     a +  h1(i-1,j)*a6*s(i,j)*sin2a(i,j)*( q2 )/dp
     a +  h4(i,j)*a6*2*sina2(i,j)*s(i,j)*( qc )/dz
     a +h4(i,j-1)*a6*2*sina2(i,j)*s(i,j)*( q4 )/dz

*     "r" denotes the derivative of total free energy with respect to S
*           of a given node.

      rd1=h0(i,j)*p(i)*( 2*a2+6*a3*s(i,j)+12*a4*s2(i,j) )
```

```
     a  + h1(i,  j)*a1*  (p(i+1)+p(i))/dp**2
     a  + h1(i-1,j)*a1*  (p(i-1)+p(i))/dp**2
     a  +(h4(i,j)+h4(i,j-1))*a1*2*p(i)/dz**2

        rd2=rd1+h0(i,j)*a6*sina2(i,j)/p(i)*2
     a  +       h1(i,j)*a6*( qa )**2/dp**2*p(i)
     a  +     h1(i-1,j)*a6*( q2 )**2/dp**2*p(i)
     a  +  h4(i,j)*a6*( qc )**2/dz**2*p(i)
     a  +h4(i,j-1)*a6*( q4 )**2/dz**2*p(i)

        rd=rd2+h1(i,j)*a6*sin2a(i,j)*( qa )/dp
     a  +    h1(i-1,j)*a6*sin2a(i,j)*( q2 )/dp
     a  +    h4(i,j)*2*a6*sina2(i,j)*( qc )/dz
     a  +  h4(i,j-1)*2*a6*sina2(i,j)*( q4 )/dz

*       "rd" denotes the derivative of r with respective to S of a given node.

*       The following three statements are to update S for a given node.

        if(rd.eq.0.)goto 27
        s(i,j)=w*(s(i,j)-r/rd)+(1-w)*s(i,j)
27      s2(i,j)=s(i,j)**2


        if(abs(s(i,j)-rems) .lt. coms)goto 20
        coms=abs(s(i,j)-rems)
        is=i
        js=j

*       "is" and "js" are to rember the point which has "coms".

20      continue
10      continue


        m=m+1
        if(m.gt.50) w=1.8
        if (m.gt.500) goto 51

*       "m" is the number of sweeps.

        if (coma.gt. 1.E-5) goto 99
        if (coms.gt. 1.e-5) goto 99
```

```
*       The above two statements is the criterion of convergence.
*       The following loop is to sum the total free energy.

51      f0=0.
        f1=0.
        f2=0.

        do 11 j=0,40
        do 22 i=0,40
        if (i**2+j**2 .gt. 1600) goto 22


        f0=f0+h0(i,j)*p(i)*( a2*s2(i,j)
     a  +a3*s2(i,j)*s(i,j)+a4*s2(i,j)**2 )
     a  +h0(i,j)*a6*s2(i,j)/p(i)*sina2(i,j)
        if ((i+1)**2+j**2 .gt. 1600) goto 24

        f1=f1+h1(i,j)*0.5*( p(i+1)+p(i) )
     a  *a1*( s(i+1,j)-s(i,j) )**2/dp**2
     a  +h1(i,j)*a6*0.5*(  p(i+1)*s2(i+1,j)+p(i)*s2(i,j)  )
     a  *( qa )**2/dp**2
     a  +h1(i,j)*a6*0.5*(  sin2a(i+1,j)*s2(i+1,j)
     a  +sin2a(i,j)*s2(i,j)  )*( qa )/dp

24      if (i**2+(j+1)**2 .gt.1600) goto 22

        f2=f2+h4(i,j)*a1*p(i)
     a  *( s(i,j+1)-s(i,j) )**2/dz**2
     a  +h4(i,j)*a6*0.5*p(i)*( s2(i,j+1)+s2(i,j) )
     a  *( qc )**2/dz**2
     a  +h4(i,j)*a6*(  sina2(i,j+1)*s2(i,j+1)
     a  +sina2(i,j)*s2(i,j)  )
     a  *( qc )/dz



22      continue
11      continue



        fb=12.56*dp*dz*(f0+f1+f2)

        f=fb+fs
```

```
      if(f.gt.remf) goto 30
      remf=f
      x=x+0.01
      if(x.gt.1.) goto 30
      m=0
      goto 99

*     The above paragraph is to compare total free energy of different shape.
*     The following paragraph is to arrange data of S field in the required form
*           of ploting program.

30    write (9,*) 4.0
      write (9,*) 0.1
      write (9,*) 81
      s(0,40)=0.
      s(40,0)=0.4
      DO 101 j=40,0,-1
      DO 102 i=40,0,-1
      write (9,*) s(i,j)
102   CONTINUE
      do 103 i1=1,40
      write (9,*) s(i1,j)
103   continue
101   CONTINUE
      do 104 j=1,40
      do 105 i=40,0,-1
      write (9,*) s(i,j)
105   continue
      do 106 i1=1,40
      write (9,*) s(i1,j)
106   continue
104   continue

      close (9)
      stop


      END
```